MATERIALS SCIENCE

Biomimetic enzyme cascade reaction system in microfluidic electrospray microcapsules

Huan Wang*, Ze Zhao*, Yuxiao Liu, Changmin Shao, Feika Bian, Yuanjin Zhao†

Mimicking subcellular compartments containing enzymes in organisms is considered a promising approach to substitute for missing or lost cellular functions. Inspired by the multicompartment structures of cellular architectures, we present a novel multienzyme system based on hollow hydrogel microcapsules with flexible enzymatic inverse opal particles. Benefiting from the precise operation capability of the microfluidic electrospray and the remarkable structural color marks in the inverse opal particles, we developed a multienzyme system with controllable number, type, and spatial arrangement of the encapsulated enzymes. The hydrogel shells also could improve enzyme stability against proteolysis in the system. The multienzyme system containing alcohol oxidase and catalase could act as a cascade biocatalyst and reduce alcohol levels in media, providing an alternative antidote and prophylactic for alcohol intoxication. These features indicated that our strategy provides an ideal enzyme cascade reaction system for complex biocatalysis and biomimetic functions of some organelles or organs.

INTRODUCTION

Enzymes are powerful biocatalysts mediating all the biological processes for living organisms. In these processes, many kinds of enzymes play their roles simultaneously. A key step in eukaryote evolution was the development of multicompartment subcellular organelles and a capacity for positional assembly, a system that minimizes the diffusion of intermediates among the enzymes and enhances the overall efficiency and specificity of bioreactions. Multiple enzymes in these unique internal structures provide eukaryotic cells with the ability for spatiotemporal control over multistep metabolic reactions. Inspired by the multienzyme architecture in eukaryotic cells, considerable attention and effort has been devoted to creating engineered enzyme cascade reaction systems with synergic and complementary functions based on liposomes or polymersomes (*1*, *2*), polymer-based capsules (*3*, *4*), and Pickering emulsions (*5*–*7*). These systems have important applications in enzyme replacement therapy (*8*, *9*), biological detoxification (*10*), chemical synthesis (*11*–*14*), and sensors (*15*, *16*). However, because of the relatively simple structure of these enzyme microcarriers, it has been difficult to control the number, type, and spatial arrangement of enzymes in these systems, a limitation that also causes difficulty in quantification control of the cascade reaction and decreases the efficiency of the biological catalysts. In addition, most of the recent enzyme microcarrier systems also suffer from inadequate translational capability and insufficient enzyme stability against proteolysis (*17*). Thus, the construction of robust microcarriers as sustainable multienzyme systems with spatiotemporally controlled functions is still anticipated.

Here, inspired by the multicompartment structures of eukaryotic cellular architecture, we present a novel multienzyme system with the desired features based on microfluidic electrospray hollow hydrogel microcapsules with flexible and mobile enzymatic inverse opal particle encapsulation. Microfluidics is an advanced technology for executing precise operations on small quantities of fluids within integrated flow channels, which is valuable for synthesizing functional microparticles or microcapsules with tunable sizes, morphologies, and compartments for different applications (*18*–*22*). Inverse opals (*23*–*26*) are a kind of structural material (*27*–*32*) with three-dimensionally (3D) ordered macroporous structure, which could provide huge specific surface areas for enzyme immobilization and interconnected channels for the access of the substrates (*33*). Thus, it is conceivable that the combination of microfluidic-synthesized multicompartment microcapsules and the enzymatic inverse opal particles would form an unprecedented biocatalyst system with specific functions of the enzyme cascade reaction, as shown in Fig. 1A. Because of the precise operation capability of the microfluidic electrospray technique (*34*–*39*) and the remarkable structural color marks in the enzymatic inverse opal particles, the number, type, and spatial arrangement of the encapsulated enzymes in each biocatalyst system can be controlled effectively to improve the efficiency of the cascade reaction. In addition, with the protection of the hydrogel shells, the translational capability and enzyme stability against proteolysis could also be promoted (*40*). We demonstrate that the multienzyme microcapsule system containing alcohol oxidase (AOx) and catalase (Cat) could act as a cascade biocatalyst and reduce alcohol levels in media, providing an alternative antidote and prophylactic for alcohol intoxication.

RESULTS

In a typical experiment, inverse opal particles with different structural colors were used to immobilize different kinds of enzymes, as shown in Fig. 1B. To generate inverse opal particles, we immersed the silica colloidal crystal bead templates with high monodispersity in a precursor solution that is composed of *N*,*N*′-methylenebis(acrylamide) (Bis) and acrylamide (AAm). The precursor would fill the voids among the silica nanoparticles of the beads. After ultraviolet (UV) light irradiation, the precursor in and out of the beads was polymerized into the hydrogel. Then, the silica colloidal crystal beads, with the hydrogel in their voids, could be collected by swelling and tearing the bulk hydrogel. After removing the template silica nanoparticles by hydrofluoric acid (HF), we prepared the inverse opal hydrogel particles. To immobilize enzymes, the hydrogel particles were hydrolyzed with sodium hydroxide and activated with *N*-(3-(dimethylamino)propyl)-*N*′-ethylcarbodiimide hydrochloride crystalline (EDC) and *N*-hydroxysuccinimide (NHS), which were then mixed with an enzyme solution overnight (*41*). Finally, after gentle rinsing with buffer solutions, the enzyme-immobilized particles were obtained (fig. S1).

State Key Laboratory of Bioelectronics, School of Biological Science and Medical Engineering, Southeast University, Nanjing 210096, China.
*These authors contributed equally to this work.
†Corresponding author. Email: yjzhao@seu.edu.cn

Scanning electron microscopy (SEM) was used to characterize the microstructures of the colloidal crystal bead templates and the corresponding inverse opal particles, as shown in Fig. 2 (A and B) and fig. S2. We observed that the nanoparticles on the surface of the template beads assembled into a hexagonal close packing, and this ordered structure also extended to the inner side (fig. S2, A and B). After the precursor solution was polymerized, the hydrogel filled the voids of the beads (fig. S2C). As the inverse opal particles often shrank and collapsed after drying (fig. S2D), a higher concentration of the cross-linker was used to maintain the morphology, and the results showed that the inverse opal particles had the expected ordered macropores (Fig. 2, A and B). This structure provided the particles not only with huge specific surface area for enzyme immobilization and interconnected channels for the substrate accessing the enzymes and the products going out but also with vivid structural colors because of the periodic structure. The periodic structure of the inverse opal particles resulted in photonic band gap (PBG). Electromagnetic waves matching the frequency of the PBG were prohibited and totally reflected, and thus, the particles showed corresponding colors. Under normal incidence, the characteristic reflective peak positions λ of the inverse opal particles could be approximately estimated by the modified Bragg's law

$$\lambda = 1.633 d n_{\text{average}} \quad (1)$$

where d is the center-to-center distance of the neighboring nanopores, and n_{average} is the average refractive index of the inverse opal particles. As different particles had the same duty ratio and gel concentration, the reflective peak positions were mainly decided by the diameter of the silica nanoparticles of the colloidal crystal bead templates. Thus, a series of inverse opal particles with distinct structural colors could be obtained by using the templates with different silica nanoparticle compositions (Fig. 2, C to F, and fig. S3). This made it possible to encode different enzymes and to construct the multienzyme system for the enzyme cascade reaction. However, the dispersive distribution of the enzyme-immobilized inverse opal particles affected the transfer efficiency of the intermediates. In addition, as the particles were directly exposed to the solution, they suffered from insufficient enzyme stability against proteolysis.

To overcome these problems, we put forward the concept of organelle-inspired microcapsules for the enzyme cascade reaction.

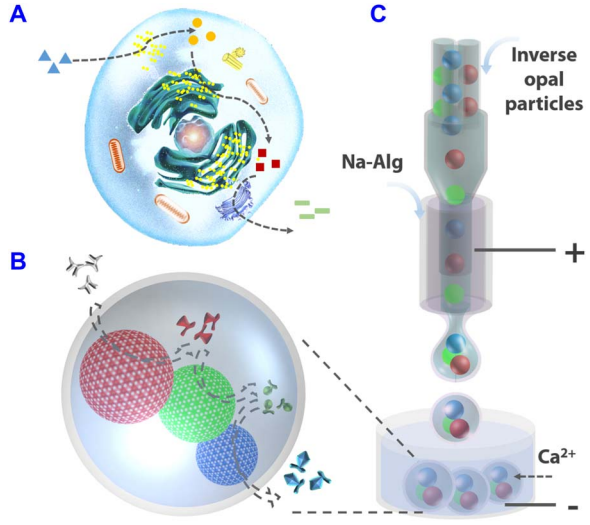

Fig. 1. Schematics of the preparation of the bioinspired microcapsules. (**A**) Schematic of the enzyme cascade reaction in a cell. (**B**) Schematic of the enzyme cascade reaction in the microcapsule encapsulated with enzyme-immobilized inverse opal particles. (**C**) Schematic of the microcapsule generation process with the microfluidic electrospray.

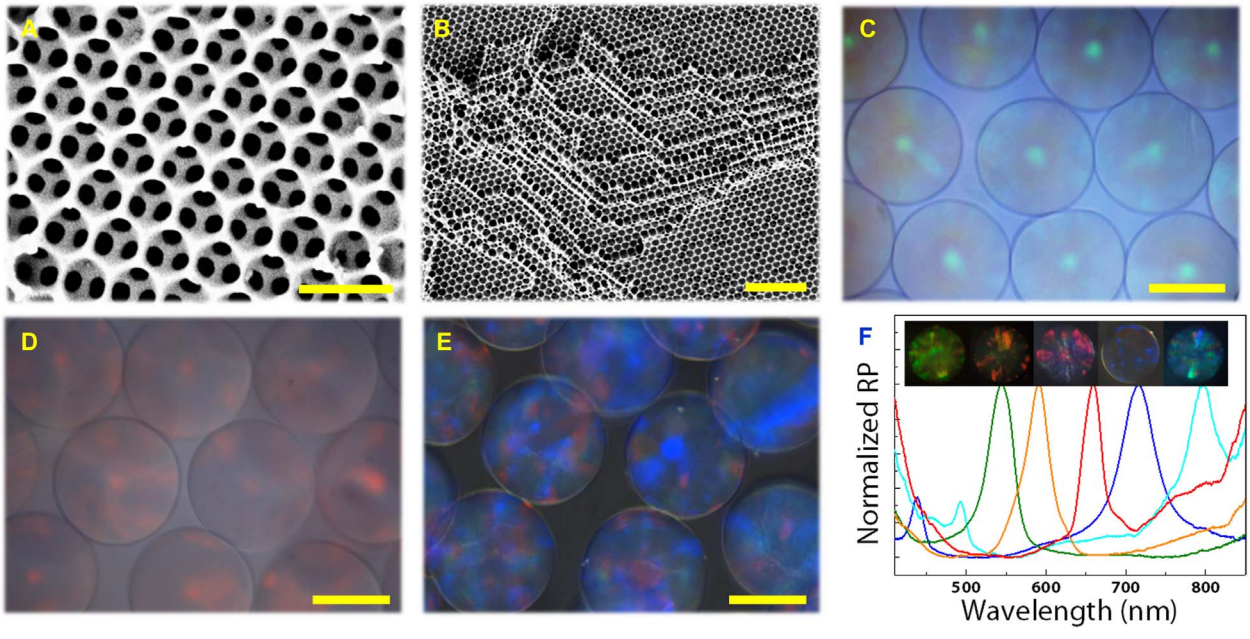

Fig. 2. SEM images and metalloscope images of the inverse opal particles. (**A**) The surface and (**B**) the inner side of an inverse opal particle with a higher concentration of the cross-linker. (**C** to **E**) Reflection images of the green, red, and blue inverse opal particles. (**F**) Reflection peaks and reflection images of five different inverse opal particles. RP, reflective percent. Scale bars, 500 nm (A), 2 μm (B), and 100 μm (C to E).

In a eukaryotic cell, many kinds of enzymes get together in small organelles and work in cascade to catalyze the substrate into production. In this process, the intermediates maintain high concentration in the small region so that the cascade reaction can be efficiently completed. Inspired by the organelles, here, we encapsulated these enzyme-immobilized inverse opal particles into microcapsules for the construction of the enzyme cascade reaction system. It was worth mentioning that the enzymes are complicated in organisms and cells and that some enzymes (such as protease and trypsin) may disturb or digest the others, resulting in reduced function or loss of the cascade reaction system (fig. S4). Thus, although the free enzymes have higher catalytic activity, enzyme immobilization and separation are necessary for the construction of a universal and stable enzyme cascade reaction. This immobilization could also avoid the adverse effects of the environment on the enzymes and prevent leakage of the enzymes from the microcapsules because of alginate hydrogel swelling. For this purpose, the inverse opal particles could not only provide huge specific surface area for enzyme immobilization but also offer interpenetrated porous structures for the enzyme catalytic reaction. In addition, because of their unique PBGs and vivid structural colors, the inverse opal particles could encode a variety of immobilized enzymes, which make the composition of the multienzyme biocatalytic system more accurate and convenient for qualitative investigation.

To realize the encapsulation, we integrated a coaxial capillary microfluidic chip with three-bore capillary injection channels using the electrospray collection device for the microcapsule generation (Fig. 1C and fig. S5, A and B). During this process, the inverse opal particles with different colors were dispersed in the sodium carboxymethylcellulose solution and flowed into a collection channel as the inner phase from the three-bore capillary injection channels (fig. S5, A and B). As the particles have density similar to their dispersed solution and have an almost dense packing in the capillary injection channels, their injection frequency could be well controlled by tailoring the flow rates of the inner phases. Then, the particles that dispersed in the inner phase were flowed into the outer phase of sodium alginate (Na-Alg) solution. Because of the hydrodynamic focusing effect, a 3D coaxial sheath flow stream of the Na-Alg solution around the inner phase flow was formed at the merging point of both flows. Under an open electric field from a voltage generator, these flows were broken up into droplets and sprayed into the gelling bath containing calcium chloride solution to instantly solidify alginate in the shell fluid before they got mixed (Fig. 3 and figs. S5, C to F, and S6). Thus, the inverse opal particles with controllable kinds and numbers could be encapsulated into the alginate hydrogel microcapsules by adjusting the flow rates of the three inner phases. Because the cavities of the microcapsules were filled with the solution, the cores were unfixed and could stay closely, which was beneficial in reducing the loss of the intermediates and in improving the efficiency of the cascade reaction.

To investigate the stability of the enzymes in the microcapsule systems, we used the microcapsules with a horseradish peroxidase (HRP)–immobilized single core as a biocatalyst and compared them with the enzyme-immobilized inverse opal particles without hydrogel shell encapsulation. The mixture of *o*-dianisidine (ODS) and hydrogen peroxide (H_2O_2) was used as the substrate. In this experiment, ODS is a kind of oxidation-reduction indicator that could be oxidized by H_2O_2 and changes to red when the HRP existed. The catalytic results of these microcapsules and particles to the substrates were shown in Fig. 4A. We found that the microcapsule system showed a lower catalytic activity than the HRP-immobilized free inverse opal particles because the shells reduced the mass transfer velocity to some extent. However, after the microcapsule systems were treated with pancreatin, they showed a higher catalytic activity than the free particles. These results indicated that the hydrogel shells of the microcapsules could protect the encapsulated enzymes on the inverse opal particles. Thus, the enzymes in the microcapsule systems could avoid being broken by the proteolysis, giving them potential for a wide range of applications.

To demonstrate the cascade reaction capability, we prepared and dispersed microcapsules with three kinds of inverse opal particles that were immobilized with β-glucosidase (β-G), glucose oxidase (GOD), and HRP in the mixture substrate of octyl β-D-glucopyranoside and ODS. In such a system, octyl β-D-glucopyranoside could be converted to glucose when it diffused to the β-G–immobilized inverse opal particles. The resultant glucose was then oxidized by GOD-immobilized inverse opal particles, which generated H_2O_2. As mentioned above, H_2O_2 could oxidize the ODS and could turn the solution into red with the assistance of the HRP-immobilized inverse opal particles. Obviously, the cascade reaction could be accomplished by microcapsules,

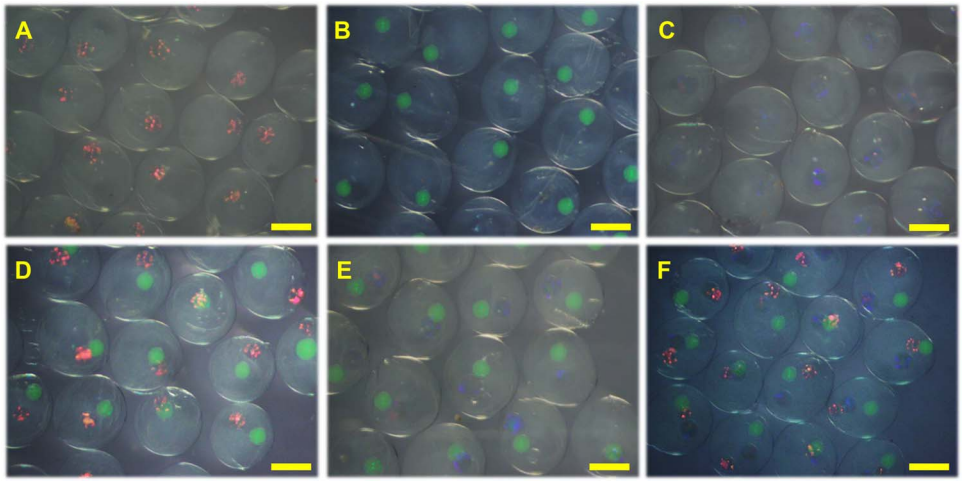

Fig. 3. The stereomicroscope images of the microcapsules with different cores. (**A** to **C**) One core. (**D** and **E**) Two cores. (**F**) Three cores. Scale bars, 400 μm.

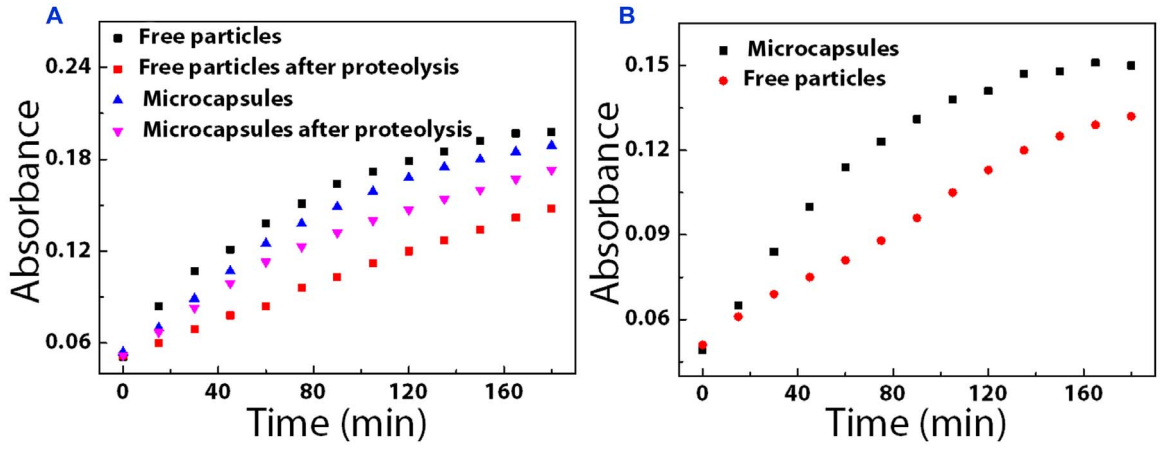

Fig. 4. The catalytic activity of the microcapsules. (**A**) Catalytic activity of HRP microcapsules and free HRP particles before and after treatment with trypsin. (**B**) Catalytic capability of the β-G–, GOD-, and HRP-immobilized inverse opal particles with and without encapsulations.

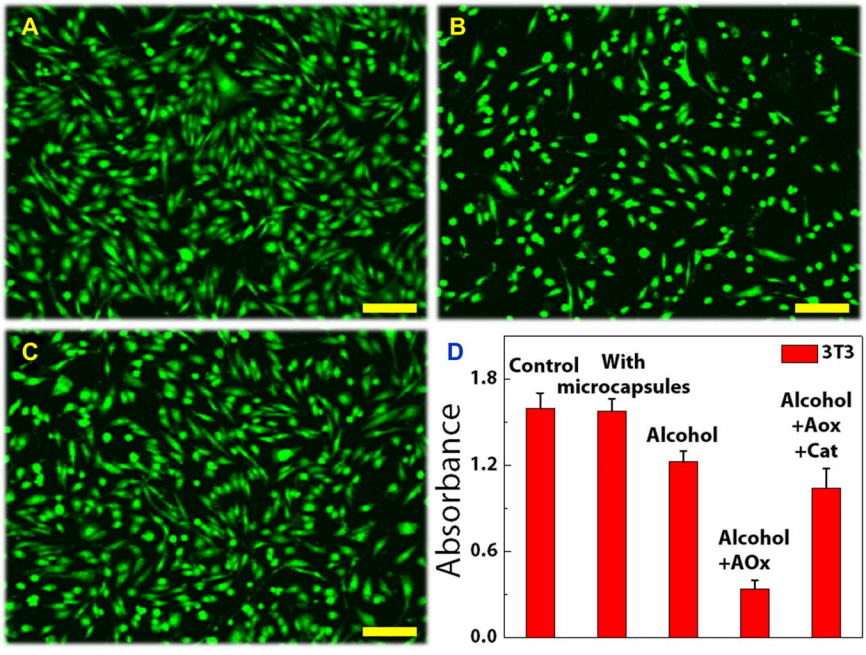

Fig. 5. Biocatalysis of the microcapsules during the cell culture. (**A** to **C**) Fluorescent staining of the cells (A) in alcohol mixed medium, (B) in the mixed medium of alcohol and AOx-encapsulated microcapsules, and (C) in the mixed medium of alcohol and AOx/Cat co-encapsulated microcapsules. (**D**) Corresponding cell viabilities. Scale bars, 50 μm.

and each step was isolated in one particle. These processes were further confirmed by the qualitative changes of the absorbance of the substrate solution, as shown in Fig. 4B. As the HRP enzyme reaction is a time-determining step of overall reaction in the cascade reaction, the velocity for single HRP enzyme reaction was a little faster than the cascade reaction. In addition, compared to the combination of the enzyme-immobilized free inverse opal particles without encapsulation, the microcapsule system showed much higher cascade reaction efficiency. This was attributed to the shorter distance among the inverse opal particles in the microcapsules so that the mass transfer could be faster and the efficiency of the whole reaction could be improved. These results indicated that the microcapsules were more stable and efficient than the free particles and free enzymes, and thus, they could be used as a new kind of enzyme cascade reaction system in the biomedical and biocatalytic fields.

To further demonstrate the practical applications of the multienzyme microcapsule system, we used it to mimic hepatocytes to accelerate the process of alcohol metabolism. Alcohol consumption is a universal culture for over thousands of years and plays an essential role in social situations. However, many organ injuries and social problems should be addressed because some people are stuck with liver dysfunction, lack certain enzymes for alcohol metabolism, and experience excessive consumption (*42*). Thus, it is crucial to construct a simple unit to mimic liver cells for alcohol detoxification. Here, we

constructed microcapsules with two kinds of inverse opal particles that were immobilized with Cat and AOx, and demonstrated their capability in the process of alcohol metabolism. To study the alcohol antidote performance, we used 3T3 cells to coculture with these microcapsules, and the results were shown in Fig. 5. In this process, the AOx could convert the alcohol into toxic H_2O_2, and H_2O_2 in turn inactivated the AOx, while the Cat could degrade H_2O_2 into H_2O and O_2, which not only eliminated the toxicity but also provided O_2 for alcohol oxidation. Thus, cell viabilities in the multienzyme microcapsule system were higher than those in the AOx-encapsulated system. It was worth mentioning that although the metabolism toxic product of H_2O_2 was eliminated in the multienzyme microcapsule system, another toxic product of acetaldehyde still existed because of the lack of aldehyde dehydrogenase (ALD) (fig. S7A). The low solubility and activity of ALD [about 70 U/ml in phosphate-buffered saline (PBS), much lower than AOx (1400 U/ml) and Cat (3000 U/ml)] restricted it to be immobilized to the particles with sufficient quantity. Although the AOx-Cat-ALD system could demonstrate such cascade reaction with microcapsules 20-fold more than the other enzyme cascade reaction (fig. S7B), it was still not applicable for cell coculture because of its insufficient activity. Thus, the microcapsules within AOx and Cat can complete elementary detoxification of alcohol, and thorough detoxification may happen when sufficiently active ALD is available for the construction of the microcapsules within AOx, Cat, and ALD.

DISCUSSION

We have developed a bioinspired multienzyme system for the enzyme cascade reaction. This multienzyme system was composed of the hydrogel shell and flexible and mobile enzyme-immobilized inverse opal particles. The inverse opal structure of the particles could not only provide huge specific area for the enzyme immobilization and mass transfer but also form vivid colors to encode different kinds of enzymes. The precise operation capability of the microfluidic electrospray resulted in controllable number, type, and spatial arrangement of the encapsulated enzyme particles. The shell of the microcapsules could hold the particles together in the interior and protect them from proteolysis. It was demonstrated that the multienzyme microcapsule system encapsulated with Cat- and AOx-immobilized inverse opal particles could effectively mimic hepatocytes for elementary alcohol detoxification. These features indicated that our strategy could provide an ideal enzyme cascade reaction system for complex biocatalysis.

Although mimicking the biological process has distinct advantages, some aspects of the multienzyme system are worth improving. First, for the design of the microcapsules, intelligent hydrogel shells that could regulate the import and export of different actives as the cell membranes would improve the efficiency of the catalytic reaction. Second, as the enzymes for cascade reaction have different environmental requirements, they require integration or decoration of different chemical groups within the enzyme-immobilized inverse opal particles to simulate the working environments of biological enzymes and to achieve high actives of enzymes. Third, to realize complex and bionic catalytic processes, we needed to study more biological enzymes and integrate them into the system. With these subsequent efforts, the multienzyme system is expected to act on biomimetic functions of some organelles or organs and even beyond the natural route.

MATERIALS AND METHODS

Materials

EDC, NHS, Bis, AAm, 2-hydroxy-2-methylpropiophenone (HMPP), tetramethylethylenediamine (TEMED), Na-Alg, sodium carboxymethylcellulose, β-G, GOD, Cat, AOx, ALD, nicotinamide adenine dinucleotide (NAD), octyl β-D-glucopyranoside, ODS, and octadecyltrichlorosilane (OTS) were obtained from Sigma-Aldrich. HRP, amylase, urease, H_2O_2, reduced form of NAD (NADH), and HF were bought from Aladdin Industrial Co. Ltd. Sodium hydroxide, *n*-hexane, and ethanol were purchased from Sinopharm Chemical Reagent Co. Ltd. SiO_2 nanoparticles in different sizes were obtained from Nanjing Nanorainbow Biotechnology Co. Ltd. Dulbecco's modified Eagle's medium (DMEM)/F12, Hanks' balanced salt solution, and fetal bovine serum (FBS) were acquired from Worthington Industries. Other reagents were of analytical grade or higher, and all the reagents were used as received. Water used in all experiments was purified using a Milli-Q Plus 185 water purification system (Millipore) with resistivity higher than 18 megohms·cm.

Experimental design

Microfluidic chip construction

The capillary microfluidic device was constructed by coaxially assembling two round capillaries (World Precision Instruments Inc.) on a glass slide. The inner capillary was tapered with a laboratory portable Bunsen burner (Honest MicroTorch) to reach an orifice inner diameter of ~250 μm. The outer diameter and inner diameter of the outer capillary were 1000 and 580 μm, respectively. The inner wall of the outer capillary was immersed in the OTS for 20 s to wet the inner wall completely and then incubated for 30 min for further hydrophobic treatment. After this, the solution was blown out with nitrogen. Then, the capillaries were coaxially assembled and a transparent epoxy resin (Devcon 5 Minute Epoxy) was used to seal the tubes where required.

Fabrication of template silica colloidal crystal beads

The silica colloidal crystal beads were generated using the droplet template method that we reported. Briefly, the nanoparticles and silicon oil were injected into the microfluidic chip through two different channels, as inner phase and outer phase. The concentration of the nanoparticles was 13 weight % (wt %), and the flow rates of the oil and water phases were 3 and 0.5 ml/hour, respectively. When the system was running, the inner phase was cut into droplets by the outer phase when they met in the microfluidic channel. A box with high-viscosity silicon oil was used to collect the droplets. Then, the box was transferred to oven at 75°C overnight to dry the droplets and the silica nanoparticles self-assembled into ordered lattices during the evaporation of water. After that, the silica colloidal crystal beads were gently washed with *n*-hexane to remove the residual silicon oil. Last, the silica colloidal crystal beads were calcined at 800°C for 4 hours to enhance their mechanical strength. The reflection spectra of the silica colloidal crystal beads were measured using a metalloscope (Olympus BX51) with a fiber-optic spectrometer (QE65000, Ocean Optics), and the photographs of the silica colloidal crystal beads were taken using a metalloscope (Olympus BX51) with a charge-coupled device camera (Media Cybernetics Evolution MP 5.0). SEM (Hitachi, S-300N) was used to characterize the microstructures of the silica colloidal crystal beads.

Fabrication of inverse opal hydrogel particles

AAm and Bis were dissolved in deionized water (mass ratio, 29:1) and then mixed with HMPP (volume ratio, 99:1) to obtain the pregel. The template colloidal crystal beads were immersed in the pregel

solution so that the voids of the beads could be filled with the pregel. After polymerization by UV light irradiation, the beads with gel were stripped from the bulk and the silica template were removed by HF. The microstructures of the inverse opal hydrogel particles were also characterized by SEM. To bind with enzymes, the inverse opal particles were hydrolyzed with 10% TEMED and 0.1 M NaOH. After activation by EDC and NHS, the enzymes (in PBS) were cross-linked with the inverse opal hydrogel particles. Fluorescein isothiocyanate–bovine serum albumin was used to mimic the enzyme distribution in the inverse opal particles.

Fabrication of the multienzyme microcapsule system

The multienzyme microcapsule system was prepared using a coaxial capillary microfluidic chip with three-bore capillary injection channels integrated with the electrospray collection device. The inverse opal particles were dispersed in 2 wt % sodium carboxymethylcellulose solution and used as inner phase, and 2 wt % Na-Alg solution was used as outer phase. Voltages (5.2 kV) from a voltage generator were used to provide electric field. Because of the hydrodynamic focusing effect, the outer phase formed sheath flow stream around the inner phase and then was broken up into microdrops by the electric field. The microdrops were collected using a container with 2 wt % calcium chloride solution, and the alginate shell was gelled. Thus, the inverse opal particles were packaged in the microcapsules as position-free cores.

Reaction of the microcapsules with HRP-immobilized single core

The mixture of ODS (0.5 g/liter) and 0.3% H_2O_2 was used as the substrate of the microcapsules with HRP-immobilized single core, and about 150 microcapsules treated with trypsin were used for biocatalysis. To monitor the reaction process, the absorbance of the substrate was monitored with a microplate reader (Synergy|HTX) every 15 min at 460 nm. About 150 free particles immobilized with HRP were used as control.

Reaction of the microcapsules immobilized with β-G, GOD, and HRP

The mixture of ODS (0.5 g/liter) and octyl β-D-glucopyranoside (25 g/liter) was used as the substrate of the microcapsules immobilized with β-G, GOD, and HRP, and about 150 microcapsules were used for biocatalysis. To monitor the reaction process, the absorbance of the substrate was monitored with a microplate reader every 15 min at 460 nm. Free particles immobilized with β-G, GOD, and HRP were used as control.

Reaction of the microcapsules immobilized with AOx and Cat

The mixture of DMEM (high level of glucose in medium, with 10% FBS) and 3% alcohol was used as the substrate of the microcapsules immobilized with Cat and AOx. The 3T3 cells with the microcapsules were cultured in the substrate for 1 hour. To monitor cell viability, the cells were treated with DMEM containing MTT (0.5 g/liter) for 3 hours. Then, DMEM was replaced with dimethyl sulfoxide. After gentle shaking, the solution was monitored with a microplate reader at 490 nm. To observe changes in cell morphology, the cocultured cells were dyed with calcein. As controls, cells cocultured without alcohol, with microcapsules but without enzymes, or with microcapsules containing only AOx were monitored simultaneously.

Reaction of the microcapsules immobilized with AOx, Cat, and ALD

The mixture of 3% alcohol and 10 mM NAD was used as the substrate of the microcapsules immobilized with AOx, Cat, and ALD, and about 3000 microcapsules were used for biocatalysis. The ALD could transform NAD to NADH, and NADH has an absorption peak at 340 nm. Thus, the cascade reaction was detected by monitoring the change of the optical density of the solution at 340 nm every 15 min.

SUPPLEMENTARY MATERIALS

Supplementary material for this article is available at http://advances.sciencemag.org/cgi/content/full/4/6/eaat2816/DC1

fig. S1. The confocal laser scanning microscopy images of the immobilized protein in the inverse opal particles.
fig. S2. SEM image characterization.
fig. S3. Optical image characterization.
fig. S4. The effects of trypsin on the enzyme cascade reaction.
fig. S5. The schematic of the microfluidic chip, real-time images of microcapsule generation, and the relationship between the diameter of the microcapsules and voltage.
fig. S6. The image of dissected microcapsules.
fig. S7. The cytotoxicity of different media and cascade reaction of alcohol.

REFERENCES AND NOTES

1. R. J. R. W. Peters, M. Marguet, S. Marais, M. W. Fraaije, J. C. M. van Hest, S. Lecommandoux, Cascade reactions in multicompartmentalized polymersomes. *Angew. Chem. Int. Ed. Engl.* **53**, 146–150 (2014).
2. X. Liu, P. Formanek, B. Voit, D. Appelhans, Functional cellular mimics for the spatiotemporal control of multiple enzymatic cascade reactions. *Angew. Chem. Int. Ed.* **56**, 16233–16238 (2017).
3. L. Hosta-Rigau, M. J. York-Duran, Y. Zhang, K. N. Goldie, B. Städler, Confined multiple enzymatic (cascade) reactions within poly(dopamine)-based capsosomes. *ACS Appl. Mater. Interfaces* **6**, 12771–12779 (2014).
4. M. Godoy-Gallardo, C. Labay, V. D. Trikalitis, P. J. Kempen, J. B. Larsen, T. L. Andresen, L. Hosta-Rigau, Multicompartment artificial organelles conducting enzymatic cascade reactions inside cells. *ACS Appl. Mater. Interfaces* **9**, 15907–15921 (2017).
5. Z. Chen, H. Ji, C. Zhao, E. Ju, J. Ren, X. Qu, Individual surface-engineered microorganisms as robust Pickering interfacial biocatalysts for resistance-minimized phase-transfer bioconversion. *Angew. Chem. Int. Ed.* **54**, 4904–4908 (2015).
6. J. Shi, X. Wang, W. Zhang, Z. Jiang, Y. Liang, Y. Zhu, C. Zhang, Synergy of Pickering emulsion and sol-gel process for the construction of an efficient, recyclable enzyme cascade system. *Adv. Funct. Mater.* **23**, 1450–1458 (2013).
7. C. Wu, S. Bai, M. B. Ansorge-Schumacher, D. Y. Wang, Nanoparticle cages for enzyme catalysis in organic media. *Adv. Mater.* **23**, 5694–5699 (2011).
8. Y. Liu, J. Du, M. Yan, M. Y. Lau, J. Hu, H. Han, O. O. Yang, S. Liang, W. Wei, H. Wang, J. Li, X. Zhu, L. Shi, W. Chen, C. Ji, Y. Lu, Biomimetic enzyme nanocomplexes and their use as antidotes and preventive measures for alcohol intoxication. *Nat. Nanotechnol.* **8**, 187–192 (2013).
9. A. Zakharchenko, N. Guz, A. M. Laradji, E. Katz, S. Minko, Magnetic field remotely controlled selective biocatalysis. *Nat. Catal.* **1**, 73–81 (2018).
10. Y. Zhang, M. Baekgaard-Laursen, B. Städler, Small subcompartmentalized microreactors as support for hepatocytes. *Adv. Healthc. Mater.* **6**, 1601141 (2017).
11. S. K. Kuk, R. K. Singh, D. H. Nam, R. Singh, J.-K. Lee, C. B. Park, Photoelectrochemical reduction of carbon dioxide to methanol through a highly efficient enzyme cascade. *Angew. Chem. Int. Ed.* **56**, 3827–3832 (2017).
12. Y. Zhang, Q. Wang, H. Hess, Increasing enzyme cascade throughput by pH-engineering the microenvironment of individual enzymes. *ACS Catal.* **7**, 2047–2051 (2017).
13. J. H. Schrittwieser, S. Velikogne, M. Hall, W. Kroutil, Artificial biocatalytic linear cascades for preparation of organic molecules. *Chem. Rev.* **118**, 270–348 (2018).
14. F. Rudroff, M. D. Mihovilovic, H. Gröger, R. Snajdrova, H. Iding, U. T. Bornscheuer, Opportunities and challenges for combining chemo- and biocatalysis. *Nat. Catal.* **1**, 12–22 (2018).
15. Y.-S. Li, W.-P. Liu, X.-F. Gao, D.-D. Chen, W.-G. Li, Immobilized enzymatic fluorescence capillary biosensor for determination of sulfated bile acid in urine. *Biosens. Bioelectron.* **24**, 538–544 (2008).
16. Y.-S. Li, Y.-D. Du, T.-M. Chen, X.-F. Gao, A novel immobilization multienzyme glucose fluorescence capillary biosensor. *Biosens. Bioelectron.* **25**, 1382–1388 (2010).
17. N. Gao, T. Tian, J. Cui, W. Zhang, X. Yin, S. Wang, J. Ji, G. Li, Efficient construction of well-defined multicompartment porous systems in a modular and chemically orthogonal fashion. *Angew. Chem. Int. Ed.* **56**, 3880–3885 (2017).
18. L. Shang, Y. Cheng, Y. Zhao, Emerging droplet microfluidics. *Chem. Rev.* **117**, 7964–8040 (2017).
19. Y. Yu, F. Fu, L. Shang, Y. Cheng, Z. Gu, Y. Zhao, Bioinspired helical microfibers from microfluidics. *Adv. Mater.* **29**, 1605765 (2017).

20. A. M. Klein, L. Mazutis, I. Akartuna, N. Tallapragada, A. Veres, V. Li, L. Peshkin, D. A. Weitz, M. W. Kirschner, Droplet barcoding for single-cell transcriptomics applied to embryonic stem cells. *Cell* **161**, 1187–1201 (2015).
21. E. Z. Macosko, A. Basu, R. Satija, J. Nemesh, K. Shekhar, M. Goldman, I. Tirosh, A. R. Bialas, N. Kamitaki, E. M. Martersteck, J. J. Trombetta, D. A. Weitz, J. R. Sanes, A. K. Shalek, A. Regev, S. A. McCarroll, Highly parallel genome-wide expression profiling of individual cells using nanoliter droplets. *Cell* **161**, 1202–1214 (2015).
22. X. Xie, W. Zhang, A. Abbaspourrad, J. Ahn, A. Bader, S. Bose, A. Vegas, J. Lin, J. Tao, T. Hang, H. Lee, N. Iverson, G. Bisker, L. Li, M. S. Strano, D. A. Weitz, D. G. Anderson, Microfluidic fabrication of colloidal nanomaterials-encapsulated microcapsules for biomolecular sensing. *Nano Lett.* **17**, 2015–2020 (2017).
23. C. Liu, H. Ding, Z. Wu, B. Gao, F. Fu, L. Shang, Z. Gu, Y. Zhao, Tunable structural color surfaces with visually self-reporting wettability. *Adv. Funct. Mater.* **26**, 7937–7942 (2016).
24. F. Fu, Z. Chen, Z. Zhao, H. Wang, L. Shang, Z. Gu, Y. Zhao, Bio-inspired self-healing structural color hydrogel. *Proc. Natl. Acad. Sci. U.S.A.* **114**, 5900–5905 (2017).
25. J. Ge, Y. Yin, Responsive photonic crystals. *Angew. Chem. Int. Ed.* **50**, 1492–1522 (2011).
26. W. Zhang, N. Gao, J. Cui, C. Wang, S. Wang, G. Zhang, X. Dong, D. Zhang, G. Li, AIE-doped poly(ionic liquid) photonic spheres: A single sphere-based customizable sensing platform for the discrimination of multi-analytes. *Chem. Sci.* **8**, 6281–6289 (2017).
27. M. Li, F. He, Q. Liao, J. Liu, L. Xu, L. Jiang, Y. Song, S. Wang, D. Zhu, Ultrasensitive DNA detection using photonic crystals. *Angew. Chem. Int. Ed.* **47**, 7258–7262 (2008).
28. L. Shang, Z. Gu, Y. Zhao, Structural color materials in evolution. *Mater. Today* **19**, 420–421 (2016).
29. L. Shang, F. Fu, Y. Cheng, H. Wang, Y. Liu, Y. Zhao, Z. Gu, Photonic crystal microbubbles as suspension barcodes. *J. Am. Chem. Soc.* **137**, 15533–15539 (2015).
30. F. Fu, L. Shang, F. Zheng, Z. Chen, H. Wang, J. Wang, Z. Gu, Y. Zhao, Cells cultured on core–shell photonic crystal barcodes for drug screening. *ACS Appl. Mater. Interfaces* **8**, 13840–13848 (2016).
31. J.-G. Park, W. B. Rogers, S. Magkiriadou, T. Kodger, S.-H. Kim, Y.-S. Kim, V. N. Manoharan, Photonic-crystal hydrogels with a rapidly tunable stop band and high reflectivity across the visible. *Opt. Mater. Express* **7**, 253–263 (2017).
32. S. Y. Lee, J. Choi, J.-R. Jeong, J. H. Shin, S.-H. Kim, Magnetoresponsive photonic microspheres with structural color gradient. *Adv. Mater.* **29**, 1605450 (2017).
33. H. Wang, H. Gu, Z. Chen, L. Shang, Z. Zhao, Z. Gu, Y. Zhao, Enzymatic inverse opal hydrogel particles for biocatalyst. *ACS Appl. Mater. Interfaces* **9**, 12914–12918 (2017).
34. Y. Song, Y. K. Chan, Q. Ma, Z. Liu, H. C. Shum, All-aqueous electrosprayed emulsion for templated fabrication of cytocompatible microcapsules. *ACS Appl. Mater. Interfaces* **7**, 13925–13933 (2015).
35. D. K. Nguyen, Y. M. Son, N.-E. Lee, Hydrogel encapsulation of cells in core-shell microcapsules for cell delivery. *Adv. Healthc. Mater.* **4**, 1537–1544 (2015).
36. S. Zhao, P. Agarwal, W. Rao, H. Huang, R. Zhang, Z. Liu, J. Yu, N. Weisleder, W. Zhang, X. He, Coaxial electrospray of liquid core–hydrogel shell microcapsules for encapsulation and miniaturized 3D culture of pluripotent stem cells. *Integr. Biol.* **6**, 874–884 (2014).
37. H. Chen, Y. Zhao, Y. Song, L. Jiang, One-step multicomponent encapsulation by compound-fluidic electrospray. *J. Am. Chem. Soc.* **130**, 7800–7801 (2008).
38. H. Doméjean, M. de la Motte Saint Pierre, A. Funfak, N. Atrux-Tallau, K. Alessandri, P. Nassoy, J. Bibette, N. Bremond, Controlled production of sub-millimeter liquid core hydrogel capsules for parallelized 3D cell culture. *Lab Chip* **17**, 110–119 (2017).
39. T. Matsuura, T. Maruyama, Hollow phosphorylcholine polymer vesicles prepared by a coaxial electrospray technique. *Colloid Polym. Sci.* **295**, 1251–1256 (2017).
40. M. Figliuzzi, T. Plati, R. Cornolti, F. Adobati, A. Fagiani, L. Rossi, G. Remuzzi, A. Remuzzi, Biocompatibility and function of microencapsulated pancreatic islets. *Acta Biomater.* **2**, 221–227 (2006).
41. D. Arunbabu, A. Sannigrahi, T. Jana, Photonic crystal hydrogel material for the sensing of toxic mercury ions (Hg^{2+}) in water. *Soft Matter* **7**, 2592–2599 (2011).
42. J. I. Garaycoechea, G. P. Crossan, F. Langevin, L. Mulderrig, S. Louzada, F. Yang, G. Guilbaud, N. Park, S. Roerink, S. Nik-Zainal, M. R. Stratton, K. J. Patel, Alcohol and endogenous aldehydes damage chromosomes and mutate stem cells. *Nature* **553**, 171–177 (2018).

Acknowledgments

Funding: This work was supported by The National Key Research and Development Program of China (2017YFA0700404), the National Science Foundation of China (grant nos. 21473029 and 51522302), the NSAF Foundation of China (grant no. U1530260), the Scientific Research Foundation of Southeast University, and the Scientific Research Foundation of Graduate School of Southeast University. **Author contributions:** Y.Z. conceived the idea and designed the experiment. H.W. and Z.Z. carried out the experiments. H.W., Y.L., and Y.Z. analyzed data and wrote the paper. C.S. and F.B. contributed to the scientific discussion of the article. **Competing interests:** The authors declare that they have no competing interests. **Data and materials availability:** All data needed to evaluate the conclusions in the paper are present in the paper and/or the Supplementary Materials. Additional data related to this paper may be requested from the authors.

Submitted 10 February 2018
Accepted 9 May 2018
Published 15 June 2018
10.1126/sciadv.aat2816

Citation: H. Wang, Z. Zhao, Y. Liu, C. Shao, F. Bian, Y. Zhao, Biomimetic enzyme cascade reaction system in microfluidic electrospray microcapsules. *Sci. Adv.* **4**, eaat2816 (2018).

Biomimetic enzyme cascade reaction system in microfluidic electrospray microcapsules

Huan Wang, Ze Zhao, Yuxiao Liu, Changmin Shao, Feika Bian and Yuanjin Zhao

Sci Adv **4** (6), eaat2816.
DOI: 10.1126/sciadv.aat2816